Scaling of the higher-order flow harmonics: implications for initial-eccentricity models and the "viscous horizon"

Roy A. Lacey,[1, *] A. Taranenko,[1] J. Jia,[1, 2] N. N. Ajitanand,[1] and J. M. Alexander[1]

[1]*Department of Chemistry, Stony Brook University,*
Stony Brook, NY, 11794-3400, USA
[2]*Physics Department, Bookhaven National Laboratory,*
Upton, New York 11973-5000, USA
(Dated: July 30, 2018)

The scaling properties of the flow harmonics for charged hadrons v_n and their ratios $[v_n/(v_2)^{n/2}]_{n \geq 3}$, are studied for a broad range of transverse momenta (p_T) and centrality selections in Au+Au and Pb+Pb collisions at $\sqrt{s_{NN}} = 0.2$ and 2.76 TeV respectively. At relatively low p_T, these scaling properties are found to be compatible with the expected growth of viscous damping for sound propagation in the plasma produced in these collisions. They also provide important constraints for distinguishing between the two leading models of collision eccentricities, as well as a route to constrain the relaxation time and make estimates for the ratio of viscosity to entropy density η/s, and the "viscous horizon" or length-scale which characterizes the highest harmonic which survives viscous damping.

PACS numbers: 25.75.-q, 25.75.Dw, 25.75.Ld

Full characterization of the transport properties of the strongly interacting matter produced in heavy ion collisions, is a central goal of the experimental heavy ion programs at both the Relativistic Heavy Ion Collider (RHIC) and the Large Hadron Collider (LHC). Collective flow, as manifested by the anisotropic emission of particles in the plane transverse to the beam direction [1], continues to play an important role in these ongoing efforts [2–15]. This anisotropy can be characterized, as a function of particle transverse momentum p_T and collision centrality (cent) or the number of participant nucleons N_{part}, by the Fourier coefficients v_n;

$$\frac{dN}{d\phi} \propto \left(1 + \sum_{n=1} 2v_n \cos(n\phi - n\Psi_n)\right), \quad (1)$$

and by the pair-wise distribution in the azimuthal angle difference $(\Delta\phi = \phi_a - \phi_b)$ between particle pairs with transverse momenta p_T^a and p_T^b (respectively) [1, 16];

$$\frac{dN^{\text{pairs}}}{d\Delta\phi} \propto \left(1 + \sum_{n=1} 2v_n^a v_n^b \cos(n\Delta\phi)\right), \quad (2)$$

where ϕ is the azimuthal angle of an emitted particle, and Ψ_n are the azimuths of the estimated participant event planes [17, 18];

$$v_n = \langle \cos n(\phi - \Psi_n) \rangle$$
$$v_n^* = \langle \cos n(\phi - \Psi_m) \rangle, \ n \neq m, \quad (3)$$

where the brackets denote averaging over particles and events. Here, the the starred notation is used to distinguish the n-th order moments obtained relative to the m-th order event plane Ψ_m (eg. v_4^* relative to Ψ_2). For flow driven anisotropy devoid of non flow effects, the Fourier coefficients obtained with Eqs. 1 and 2 are equivalent.

Flow coefficients stem from an eccentricity-driven hydrodynamic expansion of the matter in the collision zone [6, 11, 19–23], *i.e.*, a finite eccentricity ε_n drives uneven pressure gradients in- and out of the event plane, and the resulting expansion leads to the anisotropic emission of particles about this plane. The coefficients $v_n(p_T, \text{cent})$ (for odd and even n) are sensitive to both the initial eccentricity and the specific shear viscosity η/s (*i.e.* the ratio of shear viscosity η to entropy density s) of the expanding hot plasma [6–8, 20, 24–26]. Here, it is noteworthy that, for symmetric systems, the symmetry transformation $\Psi_{RP} \to \Psi_{RP} + \pi$, dictates that the odd harmonics are zero for smooth ideal eccentricity profiles. However, the "lumpy" transverse density distributions generated in individual collisions, can result in eccentricity profiles which have no particular symmetry, so the odd harmonics are not required to be zero from event to event. Fortuitously, the pervasive assumption of a smooth eccentricity profile has hindered full exploitation of the odd harmonics until recently [27].

Because of the acoustic nature of anisotropic flow (*i.e.* it is driven by pressure gradients), a transparent way to evaluate the strength of dissipative effects is to consider the attenuation of sound waves. In the presence of viscosity, sound intensity is exponentially damped $e^{(-r/\Gamma_s)}$ relative to the sound attenuation length Γ_s. This can be expressed in terms of a perturbation to the energy-momentum tensor $T_{\mu\nu}$ [28]:

$$\delta T_{\mu\nu}(t) = \exp\left(-\frac{2}{3}\frac{\eta}{s}k^2\frac{t}{T}\right)\delta T_{\mu\nu}(0), \quad (4)$$

where viscous damping reflects the dispersion relation

for sound propagation, and the spectrum of initial (t = 0) perturbations can be associated with the harmonics of the shape deformations and density fluctuations. Here, k is the wave number for these harmonics, and t and T are the expansion time and the temperature of the plasma respectively. For a collision zone of transverse size $\bar{R}$, Eq. 4 indicates that viscous corrections for the eccentricity-driven flow harmonics with wavelengths $2\pi\bar{R}/n$ for $n \geq 1$ (*i.e.* $k \sim n/\bar{R}$), dampen exponentially as n^2. The *"viscous horizon"* or length scale $r_v = 2\pi\bar{R}/n_v$ is also linked to the order of the highest harmonic n_v which effectively survives viscous damping. That is, it separates the high frequency sound modes which are fully damped from those which are not [28]. The sound horizon $r_s = \int_{\tau_0}^{\tau_f} d\tau c_s(\tau)$, or the distance sound travels at speed $c_s(\tau)$ until flow freeze-out τ_f, sets the length scale for suppression of low frequency superhorizon modes with wavelengths $2\pi R_f/n > 2r_s$, where R_f is the transverse size at sound freeze-out. Thus, the relative magnitudes of the flow harmonics v_n can provide important constraints for pinning down the magnitude of the transport coefficients η/s and c_s, as well as the "correct" model for eccentricity determinations [28–30].

Viscous damping for sound propagation in the plasma does not indicate an explicit p_T dependence for the relative magnitudes of v_n (cf. Eq. 4). However, for a finite viscosity in the plasma, the resulting asymmetry in the energy-momentum tensor manifests as a correction to the local particle distribution (f) after freeze-out [31];

$$f = f_0 + \delta f(p_T), \qquad (5)$$

where f_0 is the equilibrium distribution and $\delta f(p_T)$ is its first order correction. The latter acts as a viscous correction and is known to reduce the magnitude of $v_2(p_T)$, especially for $p_T \gtrsim 0.7$ GeV/c [31]. The relative magnitudes of $v_n(p_T)$ are expected to be dominated by the dispersion relation for sound propagation, albeit with some influence from $\delta f(p_T)$. For relatively small values of η/s, this influence on the p_T-dependent viscous corrections would also be small. Thus, a characteristic scaling relationship between $v_{n,n\geq3}(p_T)$ and $v_2(p_T)$ might be expected.

In this letter, we investigate the scaling properties of $v_n(p_T, \mathrm{cent})$ and the ratios $\left[v_n(p_T)/(v_2(p_T))^{n/2}\right]_{n\geq3}$ for charged hadrons produced in ultrarelativistic Au+Au and Pb+Pb collisions. We find scaling patterns that: (i) validate the viscous damping expected for sound propagation in the plasma created in these collisions, (ii) provide a constraint for distinguishing between the two leading eccentricity models, *i.e.* the Glauber [32] and the factorized Kharzeev-Levin-Nardi (KLN) [33–35] models, and (iii) point to an independent and robust method to estimate η/s.

The double differential data, $v_n^*(p_T, \mathrm{cent})$ and $v_n(p_T, \mathrm{cent})$, employed in our analysis are obtained from
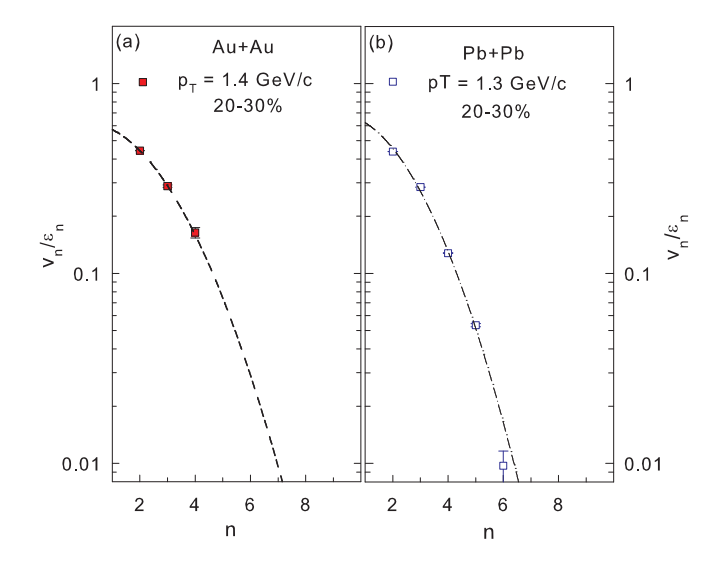

FIG. 1. v_n/ε_n vs. n for charged hadrons ($p_T \sim 1.4$ GeV/c) produced in Au+Au collisions at $\sqrt{s_{NN}} = 0.2$ TeV (a) and Pb+Pb collisions at $\sqrt{s_{NN}} = 2.76$ TeV. The v_n data are taken from Refs. [36] and [37, 38] respectively for 20-30% centrality. The curves represent fits to the data (see text).

measurements by the PHENIX collaboration, for Au+Au collisions at $\sqrt{s_{NN}} = 0.2$ TeV [18, 36], and measurements by the ATLAS collaboration for Pb+Pb collisions at $\sqrt{s_{NN}} = 2.76$ TeV [37, 38]. The Au+Au data set exploits the event plane analysis method (c.f. Eq. 3), while the Pb+Pb data set utilizes the two-particle $\Delta\phi$ correlation technique (c.f. Eq. 2), as well as the event plane method. Note as well that, due to partial error cancellation, the relative systematic errors for the ratios $v_n/(v_2)^{n/2}$ and $v_n^*/(v_2)^{n/2}$ can be smaller than the ones reported for the v_n values.

To perform validation tests for viscous damping compatible with sound propagation, the measured values of $v_n(\mathrm{cent})$, for each p_T selection, were first divided by $\varepsilon_n(\mathrm{cent})$ and then plotted as a function of n. Monte Carlo (MC) simulations were used to compute $\varepsilon_n(\mathrm{cent})$ from the two-dimensional profile of the density of sources in the transverse plane $\rho_s(\mathbf{r}_\perp)$, with weight $\omega(\mathbf{r}_\perp) = \mathbf{r}_\perp{}^n$ [29]. Figs. 1 (a) and (b) show representative examples of v_n/ε_n vs. n for charged hadrons ($p_T \sim 1.4$ GeV/c) in mid-central Au+Au and Pb+Pb collisions respectively. They confirm the exponential decrease of v_n/ε_n with n^2, expected for sound propagation. This "acoustic scaling" of v_n is further confirmed by the dashed and dot-dashed curves which indicate exponential/Gaussian fits ($Ae^{-\beta n^2}$) to the data shown.

Similar patterns were observed for a broad selection of centralities for $p_T \lesssim 3$ GeV/c. However, for the 0-5% and 5-10% most central Pb+Pb collisions, v_2/ε_2 shows significant suppression relative to the empirical trend for v_n vs. n, for other centralities shown by the curves in Fig. 1. The fractional magnitude of this suppression is
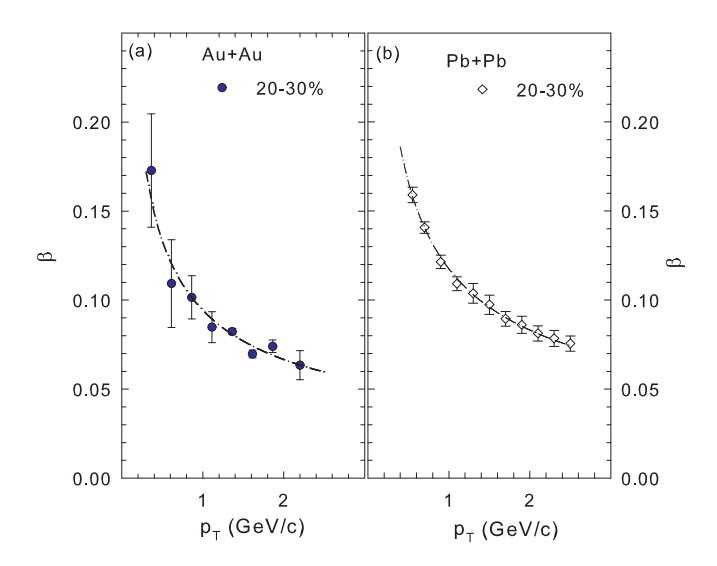
FIG. 2. β vs. p_T for 20-30% central Au+Au collisions at $\sqrt{s_{NN}} = 0.2$ TeV (a) and 20-30% central Pb+Pb collisions at $\sqrt{s_{NN}} = 2.76$ TeV (b). The dot-dashed and dashed curves indicate a $1/\sqrt{(p_T)}$ dependence for β (see text).
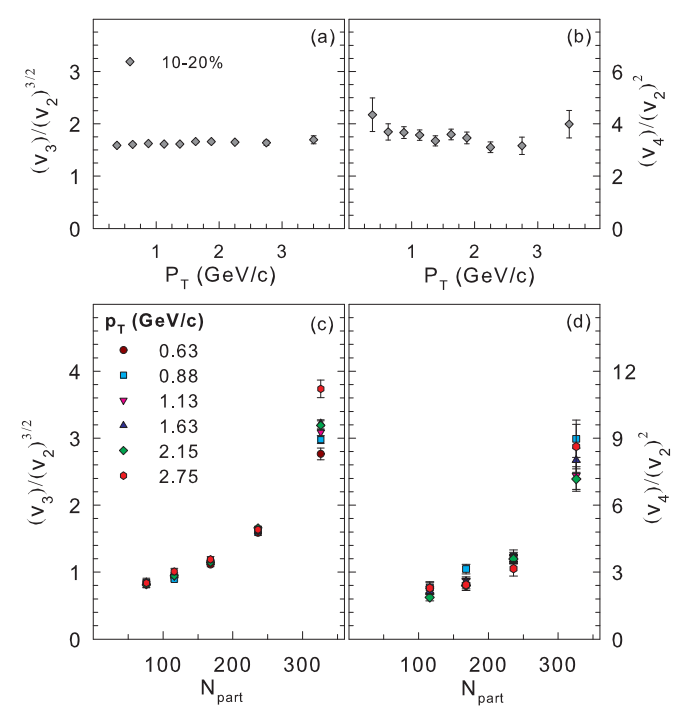

FIG. 3. $v_3/(v_2)^{3/2}$ vs. p_T (a) and $v_4/(v_2)^2$ vs. p_T for 10-20% central Au+Au collisions. The bottom panels show $v_3/(v_2)^{3/2}$ vs. N_{part} (c) and $v_4/(v_2)^2$ vs. N_{part} (d) for several p_T cuts, as indicated. The $v_{2,3,4}$ values used for these ratios are reported in Ref. [36].

essentially independent of p_T even though $v_2/\varepsilon_2 < v_3/\varepsilon_3$ for $p_T \gtrsim 2$ GeV/c. We interpret this suppression as an indication that, for the most central Pb+Pb collisions, the low frequency modes $n < 3$ exceed the superhorizon limit, i.e. $2\pi R_f/n > 2r_s$. That is, for these low frequency modes, the requirement for the maximum momentum anisotropy to develop is not met, so only a fraction of the full anisotropy is observed. For mid-central collisions, these sound modes have shorter wavelengths which make them sub-horizon. Note that $R_f = \bar{R} + r_s$, so the order n of the low frequency modes which are suppressed, can serve to constrain the sound speed.

For each centrality, exponential fits ($Ae^{-\beta n^2}$) to v_n/ε_n vs. n were also made to investigate the p_T-dependent viscous corrections attributable to $\delta f(p_T)$. Figs. 2 (a) and (b) show the p_T-dependence of the β values extracted for 20-30% central Au+Au and Pb+Pb collisions respectively; similar data trends were observed for other centralities. The dashed and dot-dashed curves in Fig. 2 show that β scales as $1/\sqrt{(p_T)}$ for both collision energies, but the values for Pb+Pb collisions are about 25% larger. This scaling is a clear indication of the influence of the relaxation time [15, 31]. Consequently it should serve as an important constraint for models.

Figure 3 shows the ratios $v_3/(v_2)^{3/2}$ and $v_4/(v_2)^2$ plotted as a function of p_T [(a) and (b)] and N_{part} [(c) and (d)] respectively, for Au+Au collisions. These ratios indicate an essentially flat dependence on p_T, but show a characteristic increase with N_{part}. The same trends are exhibited by the Pb+Pb data ($\sqrt{s_{NN}} = 2.76$ TeV) with magnitudes comparable to those for Au+Au collisions for the same range of p_T and centrality selections. We interpret the flat p_T dependence of $v_n/(v_2)^{n/2}$ [for each

cent] to be an indication that the p_T-dependent viscous corrections for v_n are dominated by the p_T-independent contributions which stem from the dispersion relation for sound propagation.

The trends for $v_4^*/(v_2)^2$ were found to be similar to those for $v_4/(v_2)^2$, but the ratios $v_4^*/(v_2)^2$ vs. N_{part} are much less steep [18]. The N_{part} dependence of $v_4^*/(v_2)^2$ and $v_4/(v_2)^2$ contrasts with the constant value of ~ 0.5 predicted for perfect fluid hydrodynamics [39, 40], and points to the important role of the higher-order eccentricity moments and their fluctuations [15, 27, 29, 41, 42]. The apparent differences between $v_4^*/(v_2)^2$ and $v_4/(v_2)^2$ are also an indication of the important role of ε_4 as a driver for v_4. That is, the expected contribution to v_4 from v_2 [$\sim (v_2)^2$] does not dominate the v_4 measurements. Note as well that $v_4 > v_4^*$ is expected because the initial eccentricity fluctuations cause Ψ_2 to fluctuate about Ψ_4.

The flat p_T dependence for $v_n/(v_2)^{n/2}$ (c.f Fig. 3) also suggests that the p_T-dependent contributions to the viscous corrections for the ratios $(v_n/\varepsilon_n)/(v_2/\varepsilon_2)^{n/2}$ essentially cancel, making them a reliable constraint for the ratios $\varepsilon_n/(\varepsilon_2)^{n/2}$ and consequently, an important route for distinguishing between different eccentricity models [29]. The solid symbols in Fig. 4 show a representative set of the experimental $v_n/(v_2)^{n/2}$ ratios which take account of the relatively small effects of acoustic suppression. The
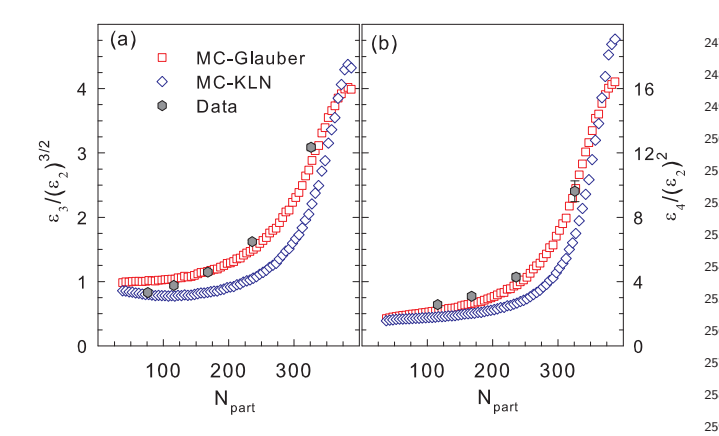
FIG. 4. Data comparisons to the calculated ratios (a) $\varepsilon_3/(\varepsilon_2)^{3/2}$ vs. N_{part} and (b) $\varepsilon_4/(\varepsilon_2)^2$ vs. N_{part} for MC-Glauber and MC-KLN initial geometries for Au+Au collisions (see text).

open symbols show the corresponding eccentricity ratios obtained for the two eccentricity models. The ε_n values for these ratios were evaluated as described earlier. Fig. 4 indicates relatively good agreement between data and the $\varepsilon_n/(\varepsilon_2)^{n/2}$ ratios, confirming the utility of $v_n/(v_2)^{n/2}$ as a constraint for distinguishing between the eccentricity models [29].

The observed scaling patterns summarized in Figs. 1 - 3 undoubtedly provide an important set of constraints for detailed comparisons to model calculations. In lieu of such calculations, we demonstrate their current utility for first rough estimates of the magnitude of η/s and the viscous horizon. To this end, we employ fits to both the Au+Au and Pb+Pb data, with the fit function $(A\sqrt{(p_T)}e^{-\frac{\beta n^2}{\sqrt{(p_T)}}}$, where the $\sqrt{(p_T)}$ factors account for the influence of $\delta f(p_T)$. These fits indicate that, relative to v_2/ε_2, the magnitude of $v_n/\varepsilon_{n,n\geq 3}$ decreases by more than a factor of 50 for $n_v \sim 7$, i.e. v_n/ε_n for $n \gtrsim 7$ are essentially completely damped. This gives the estimate $r_v = 2\pi\bar{R}/n_v \simeq 1.8$ fm for the viscous horizon in central Au+Au and Pb+Pb collisions.

The same fits allow robust extraction of the β values for Au+Au and Pb+Pb collisions. Here, it is noteworthy that the dependence of v_n/ε_n on n can provide a particularly tight constraint, because it is the relative magnitudes of v_n/ε_n which now serve to constrain β. These β values have been used to extract a first rough estimate of $4\pi\eta/s \sim 1.2$ for central Au+Au collisions for $\langle T \rangle = 220$ MeV and $t = 9$ fm [12]. This rough estimate is in reasonable qualitative agreement with the values from prior extractions [4–8, 10, 11, 14, 31, 41]. A similarly rough estimate from the Pb+Pb data ($\sqrt{s_{NN}} = 2.76$ TeV) gives a value for η/s which is approximately 25% larger (cf. the larger value for β) if we assume that the ratio T/t is roughly the same for Au+Au and Pb+Pb collisions [43]. That is, we assume that a possibly larger flow freeze-out time is compensated for, by a higher estimated mean temperature. More detailed model calculations are required to address the values of $\langle T \rangle$ and t required for a more accurate estimate of η/s. Nonetheless, our procedure clearly demonstrates the value of the relative magnitudes of v_n for extraction of η/s.

In summary, we have presented a detailed study of the scaling properties of the flow coefficients v_n and their ratios $[v_n/(v_2)^{n/2}]_{n\geq3}$, for Au+Au and Pb+Pb collisions at $\sqrt{s_{NN}} = 0.2$ and 2.76 TeV respectively. Within an empirically parametrized viscous hydrodynamical framework, these properties can be understood to be a consequence of the acoustic nature of anisotropic flow, i.e, the observed viscous damping is characteristic of sound propagation in the plasma produced in these collisions. This interpretation not only provides a straightforward constraint for distinguishing between the two leading eccentricity models, it provides a means to constrain the relaxation time and the sound speed, as well as to make independent estimates for the the averaged specific shear viscosity and the viscous horizon, via studies of the relative magnitudes of v_n. The observed scaling also has important implications for accurate decomposition of flow and jet contributions to two-particle $\Delta\phi$ correlation functions. This is because the higher-order harmonics can be expressed as a power of the high precision v_2 harmonic. It will be valuable to perform detailed viscous hydrodynamical model comparisons to v_n and $v_n/(v_2)^{n/2}$ for both identified and unidentified hadrons, as well as to establish the p_T value which signals a breakdown of these scaling patterns.

* E-mail: Roy.Lacey@Stonybrook.edu

[1] R. A. Lacey, Nucl. Phys. **A698**, 559 (2002); R. J. M. Snellings, *ibid.* **A698**, 193 (2002).

[2] M. Gyulassy and L. McLerran, Nucl. Phys. **A750**, 30 (2005).

[3] D. Molnar and P. Huovinen, Phys. Rev. Lett. **94**, 012302 (2005), arXiv:nucl-th/0404065.

[4] R. A. Lacey *et al.*, Phys. Rev. Lett. **98**, 092301 (2007).

[5] A. Adare *et al.*, Phys. Rev. Lett. **98**, 172301 (2007).

[6] P. Romatschke and U. Romatschke, Phys. Rev. Lett. **99**, 172301 (2007).

[7] Z. Xu, C. Greiner, and H. Stocker, Phys. Rev. Lett. **101**, 082302 (2008).

[8] H.-J. Drescher, A. Dumitru, C. Gombeaud, and J.-Y. Ollitrault, Phys. Rev. **C76**, 024905 (2007).

[9] E. Shuryak, Prog. Part. Nucl. Phys. **62**, 48 (2009).

[10] M. Luzum and P. Romatschke, Phys. Rev. **C78**, 034915 (2008).

[11] H. Song and U. W. Heinz, J. Phys. **G36**, 064033 (2009).

[12] K. Dusling and D. Teaney,

Phys. Rev. **C77**, 034905 (2008), arXiv:0710.5932 [nucl-th].

[13] P. Bozek and I. Wyskiel, PoS **EPS-HEP-2009**, 039 (2009), arXiv:0909.2354 [nucl-th].

[14] G. S. Denicol, T. Kodama, and T. Koide, (2010), arXiv:1002.2394 [nucl-th].

[15] R. A. Lacey *et al.*, (2010), arXiv:1005.4979 [nucl-ex].

[16] A. Mocsy and P. Sorensen, (2010), arXiv:1008.3381 [hep-ph].

[17] J.-Y. Ollitrault, Phys. Rev. **D46**, 229 (1992).

[18] A. Adare *et al.* (PHENIX), Phys. Rev. Lett. **105**, 062301 (2010), arXiv:1003.5586 [nucl-ex].

[19] U. Heinz and P. Kolb, Nucl. Phys. **A702**, 269 (2002).

[20] D. Teaney, Phys. Rev. **C68**, 034913 (2003).

[21] P. Huovinen, P. F. Kolb, U. W. Heinz, P. V. Ruuskanen, and S. A. Voloshin, Phys. Lett. **B503**, 58 (2001).

[22] T. Hirano and K. Tsuda, Phys. Rev. **C66**, 054905 (2002), arXiv:nucl-th/0205043.

[23] B. Schenke, S. Jeon, and C. Gale, (2010), arXiv:1009.3244 [hep-ph].

[24] U. W. Heinz and S. M. H. Wong, Phys. Rev. **C66**, 014907 (2002).

[25] R. A. Lacey and A. Taranenko, PoS **CFRNC2006**, 021 (2006).

[26] V. Greco, M. Colonna, M. Di Toro, and G. Ferini, (2008), arXiv:0811.3170 [hep-ph].

[27] B. Alver and G. Roland, Phys. Rev. **C81**, 054905 (2010), arXiv:1003.0194 [nucl-th].

[28] P. Staig and E. Shuryak, (2010), arXiv:1008.3139 [nucl-th].

[29] R. A. Lacey, R. Wei, N. N. Ajitanand, and A. Taranenko, (2010), arXiv:1009.5230 [nucl-ex].

[30] B. H. Alver, C. Gombeaud, M. Luzum, and J.-Y. Ollitrault, (2010), arXiv:1007.5469 [nucl-th].

[31] K. Dusling, G. D. Moore, and D. Teaney, (2009), arXiv:0909.0754 [nucl-th].

[32] M. L. Miller, K. Reygers, S. J. Sanders, and P. Steinberg, Ann. Rev. Nucl. Part. Sci. **57**, 205 (2007).

[33] D. Kharzeev and M. Nardi, Phys. Lett. **B507**, 121 (2001), arXiv:nucl-th/0012025.

[34] T. Lappi and R. Venugopalan, Phys. Rev. **C74**, 054905 (2006).

[35] H.-J. Drescher and Y. Nara, Phys. Rev. **C76**, 041903 (2007).

[36] A. Adare *et al.* (PHENIX), (2011), arXiv:1105.3928 [nucl-ex].

[37] J. Jiangyong (ATLAS), (2011), arXiv:1107.1468 [nucl-ex].

[38] ATLAS Note,ATLAS-CONF-2011-074, 2011.

[39] N. Borghini and J.-Y. Ollitrault, Phys. Lett. **B642**, 227 (2006).

[40] M. Csanad, T. Csorgo, and B. Lorstad, Nucl. Phys. **A742**, 80 (2004), arXiv:nucl-th/0310040.

[41] R. A. Lacey, A. Taranenko, and R. Wei, (2009), arXiv:0905.4368 [nucl-ex].

[42] R. A. Lacey *et al.*, Phys. Rev. **C81**, 061901 (2010), arXiv:1002.0649 [nucl-ex].

[43] B. Schenke, S. Jeon, and C. Gale, Phys. Lett. **B702**, 59 (2011), arXiv:1102.0575 [hep-ph].